Double Star Measurements at the Southern Sky with a 50 cm Reflector in 2016.

Rainer Anton

Altenholz/Kiel, Germany
e-mail: rainer.anton”at”ki.comcity.de

Abstract: A 50 cm Ritchey-Chrétien reflector was used for recordings of double stars with a CCD webcam, and measurements of 95 pairs were mostly obtained from “lucky images”, and in some cases by speckle interferometry. The image scale was calibrated with reference systems from the recently published *Gaia* catalogue of precise position data. For several pairs, deviations from currently assumed orbits were found. Some images of noteworthy systems are also presented.

Introduction

Recordings of double star images were mostly evaluated with “lucky imaging”: Seeing effects are effectively reduced by using short exposure times, and selection of only the best images for stacking, which results in virtually diffraction limited images. In addition, speckle interferometry was applied in some cases, as large numbers of speckle images were found in several recordings, caused by rather variable seeing conditions during this observing campaign. More details of these techniques are described, for example, in references [1] and [2].

The accuracy of position measurements depends on mainly three factors: the seeing, the size and resolution of the telescope, and the calibration factor of the image scale. In earlier work, the latter was based on reference systems from the literature. Here, a much more precise value was obtained with data from the *Gaia* satellite mission, which delivered star positions with unprecedented accuracy [3].

Instrumental

The 50 cm Ritchey-Chrétien telescope is located at the “*Internationale Amateursternwarte”* on a guest farm in Namibia [4], and which I have already used in 2014 for double star work [5]. The primary focal length of 4.1 m was extended by a 2x Barlow lens, resulting in an f-ratio of about f/16. Series of 1000 to 2000 images were taken with a b/w-CCD camera of type “Chameleon” (PointGrey) with exposure times ranging from less than a millisecond to several tens of msec, depending on the star brightness, on the filter being used, and on the seeing. Recordings were usually made with a red or near infrared filter, in order to reduce effects from chromatic aberrations of the Barlow lens, as well as from the seeing. Only the best frames, typically several tens and up to more than 100, were selected, registered, and stacked. The pixel size of 3.75 µm square results in a nominal resolution of 0.096 arcsec/pixel. A more accurate value was obtained with reference systems, as was already indicated above, and as will be explained in more detail below. In any case, the accuracy of position measurements is typically better by more than one order of magnitude. Images were re-sampled before stacking, as registering can be done with sub-pixel accuracy, which results in smoothening of the intensity profiles, and better definition of the peak centroids. Position angles were obtained by recording star trails with the telescope drive switched off, from which the east-west direction was determined.

The seeing was often somewhat turbulent, with frequent changes from “lucky images” to speckle images. In recordings of 9 brighter systems, up to several hundred useful speckle images were found. These were evaluated, eventually after enhancing the contrast, with the function *autocorrelation* within the program *Reduc*, made available by Florent Losse [6].

Calibration

The image scale was adjusted by using data from the *Gaia DR1* catalog, which became freely available in September 2016. For 20 systems out of the total of 95 investigated here, values for right ascension and declination of the components were found, with error margins typically smaller than one milliarcsecond, from which separations and position angles were calculated. The reference systems are marked in table 1 below with shaded lines. The *DR1* contains measurements performed in late 2014 and in 2015, but the positions refer to the epoch 2015.0. In some cases, where positions of double stars are known to rapidly change, those calculated from Gaia data were extrapolated to the epoch of my own recordings. Maximum shifts were about 0.1 degrees and 0.01 arcsec, respectively. An example is shown below. The image scale was adjusted by statistical evaluation of the residuals of the reference systems, such that the mean value and the standard deviation (s. d.) were minimized. As a result, the range of residuals extended from -0.008 to +0.009 arcsec (this can be seen in fig. 1 below), the mean was less than 0.001 arcsec, the s. d. was +/- 0.005 arcsec, and the scale factor became 0.09557 arcsec/pixel with an estimated error of less than +/- 0.1 per cent. The resulting effective resolution differs from the nominal value given above by -0.4 percent.

Results

All measurements are listed in table 1. Names, nominal positions, and magnitudes are adopted from the *WDS* [7]. Residuals of the reference systems (shaded lines) refer to *Gaia* data, as was explained above. For most other systems, in particular for binaries, residuals refer to ephemeris data from the Sixth Catalog of Orbits of Visual Binary Stars [8]. In several cases, no reasonable residuals could be given, because of too few literature data and/or too large a scatter. The table is followed by individual notes, which are numbered with RA values. Notes often refer to speckle data, which were obtained from the so-called “speckle catalog” [9].

Table 1: List of measurements. Position angles (PA) are in degrees, separations (ρ) in arc seconds. N is the number of recordings. For N > 1, measures are mean values, including results from speckle interferometry (see below). Shaded lines indicate systems, which are used for calibration of the image scale by reference to Gaia data. Residuals (Δ PA, $\Delta\rho$) are given, when reasonable. Asterisks in column “PAIR” refer to figures shown below.

PAIR	RA + Dec	MAGS	PA meas.	ρ meas.	DATE	N	Δ PA	$\Delta\rho$
SLR 1 AB	01 06.1 -46 43	4.10 4.19	83.83	0.577	2016.344	2	0.75	-0.009
H 3 27 AB	07 38.8 -26 48	4.40 4.62	318.17	9.931	2016.332	1	--	--
HU 710	07 43.0 -17 04	7.00 7.95	61.30	0. 479	2016.332	1	0.97	0.012
STF 1146	07 47.9 -12 12	5.73 7.32	338.00	1.080	2016.332	1	-0.47	0.014
SEE 91	07 55.8 -43 51	6.60 6.69	347.67	0.778	2016.332	1	--	--
BU 205 AB	08 33.1 -24 36	7.14 6.84	286.80	0.578	2016.332	1	3.36	-0.012
BU 208 AB	08 39.1 -22 40	5.37 6.81	42.50	0.794	2016.332	1	-10.56	0.189
COP 1	09 30.7 -40 28	3.91 5.12	121.60	1.017	2016.337	1	-2.64	-0.089
RST 1435	09 32.3 -40 39	5.50 8.37	102.80	1.015	2016.337	1	--	--

AC 5 AB	09 52.5 -08 06	5.43 6.41	42.08	0.494	2016.357	1	0.48	-0.030
I 173	10 06.2 -47 22	5.32 7.10	9.10	0.967	2016.337	1	-0.43	-0.009
BU 411	10 36.1 -26 41	6.68 7.77	304.70	1.320	2016.337	1	0.08	0.005
SEE 119	10 37.3 -48 14	4.13 5.76	245.60	0.429	2016.337	1	1.50	0.044
STF 1466 AB	10 43.3 +04 45	6.23 7.13	239.70	6.824	2016.357	1	--	--
R 155	10 46.8 -49 25	2.82 5.65	56.90	2.280	2016.337	1	0.37	-0.106
STF 1476	10 49.3 -04 01	7.08 7.82	16.27	2.481	2016.357	1	--	--
HJ 4383	10 53.7 -70 43	6.38 7.09	289.70	1.534	2016.359	1	--	--
R 163 A,BC	11 17.5 -59 06	7.24 7.60	58.00	1.630	2016.359	1	-0.20	-0.008
HJ 4432	11 23.4 -64 57	5.37 6.56	309.40	2.504	2016.357	1	--	--
HU 462	11 27.2 -15 39	8.42 8.53	69.30	0.413	2016.357	1	-3.64	-0.007
I 885 AB	11 28.6 -45 08	7.98 9.90	148.96	0.631	2016.337	1	9.76	0.126
HJ 4455 AB	11 36.6 -33 34	6.01 7.77	240.10	3.440	2016.357	1	--	--
COO 130	11 51.9 -65 12	4.97 7.25	157.85	1.448	2016.357	1	--	--
HLD 114	11 55.0 -56 06	7.60 7.81	169.00	3.869	2016.337	1	0.02	0.002
DUN 117 AB	12 04.8 -62 00	7.40 7.83	149.08	22.787	2016.337	1	-0.19	-0.003
HWE 72	12 13.6 -33 48	6.48 8.55	159.20	1.231	2016.357	1	--	--
BU 920	12 15.8 -23 21	6.86 8.22	307.20	1.934	2016.337	1	-0.17	0.030
BSO 8	12 24.9 -58 07	7.84 7.98	334.70	5.234	2016.342	2	0.11	0.001
DUN 252 AB	12 26.6 -63 06	1.25 1.55	111.75	3.894	2016.346	5	--	--
DUN 252 AC		1.25 4.80	202.00	90.107	2016.346	2	--	--
CPO 12 A,BC	12 28.3 -61 46	7.32 8.24	186.20	2.051	2016.337	2	-0.17	0.000
STF 1669 AB	12 41.3 -13 01	5.88 5.89	313.80	5.246	2016.370	1	--	--
STF 1670 AB *	12 41.7 -01 27	3.48 3.53	2.92	2.454	2016.332	3	-0.27	-0.003
R 207 AB	12 46.3 -68 06	3.52 3.98	53.23	1.006	2016.351	3	-7.29	0.140
DUN 126 AB	12 54.6 -57 11	3.94 4.95	16.64	34.891	2016.370	1	--	--
I 83	12 56.7 -47 41	7.39 7.68	236.57	0.859	2016.342	3	0.64	-0.004
BU 341	13 03.8 -20 35	6.25 6.51	130.50	0.380	2016.342	2	-0.33	0.003
RST 3829 Aa,Ab	13 14.9 -11 22	7.35 9.14	159.35	0.511	2016.332	2	-1.19	-0.036
SHJ 162 AB		7.11 8.12	44.29	112.661	2016.332	1	-0.21	-0.026
STF 1757 AB	13 34.3 -00 19	7.82 8.75	140.68	1.718	2016.329	2	-0.02	-0.004
BU 932 AB	13 34.7 -13 13	6.30 7.29	66.49	0.429	2016.329	1	0.66	0.009
HWE 95 AB	13 43.8 -40 11	7.51 7.85	185.20	0.926	2016.335	2	--	--
STF 1781 AB	13 46.1 +05 07	7.89 8.10	194.80	1.005	2016.329	1	-0.25	-0.007
HWE 28 AB	13 53.5 -35 40	6.27 6.38	315.40	1.010	2016.329	2	0.27	0.002
H 5 124 AE		6.27 8.65	6.84	68.303	2016.329	1	--	--
STF 1788 AB	13 55.0 -08 04	6.68 7.26	100.50	3.747	2016.329	1	0.60	0.157
SLR 19	14 07.7 -49 52	7.14 7.38	328.30	1.069	2016.331	2	-0.17	-0.052
HJ 4672	14 20.2 -43 04	5.77 7.94	301.24	3.453	2016.335	1	--	--
RHD 1 AB *	14 39.6 -60 50	-0.01 1.33	307.25	3.997	2016.347	9	1.75	-0.072
NZO 52	14 40.8 -66 57	7.87 8.54	59.22	2.193	2016.337	1	-0.13	-0.001
I 227 AB	14 56.5 -34 38	8.06 8.39	97.20	0.441	2016.332	1	2.07	-0.024
HJ 4715	14 56.5 -47 53	5.98 6.82	277.58	2.094	2016.335	1	--	--
HJ 4728	15 05.1 -47 03	4.56 4.60	63.90	1.605	2016.370	1	--	--
I 228	15 14.0 -43 48	7.98 8.24	11.20	1.353	2016.337	1	-0.34	-0.001
HJ 4753 AB	15 18.5 -47 53	4.93 4.99	298.72	0.774	2016.370	2	--	--

DUN 180 AC		4.93 6.34	129.28	22.936	2016.370	1	--	--
CPO 16 AB	15 29.5 -58 21	7.03 7.98	34.02	2.466	2016.337	1	-0.25	-0.006
HJ 4786 AB *	15 35.1 -41 10	2.95 4.45	275.66	0.829	2016.330	3	-0.74	-0.003
HJ 4825 AB,C	16 03.5 -57 47	5.20 5.76	242.07	11.085	2016.336	4	--	--
HWE 82	16 03.8 -33 04	7.71 7.86	344,80	2.317	2016.332	2	-0.07	0.009
STF 1998 AB	16 04.4 -11 22	5.16 4.87	6.14	1.097	2016.331	3	--	--
STF 1998 AC	16 04.4 -11 22	5.16 7.30	41.60	7.992	2016.331	2	0.17	0.006
STF 1999 AB	16 04.4 -11 27	7.52 8.05	98.41	11.858	2016.332	1	-0.07	-0.004
BU 120 AB	16 12.0 -19 28	4.35 5.31	2.36	1.327	2016.331	2	--	--
MTL 2 CD		6.60 7.23	55.39	2.402	2016.331	2	-0.42	0.007
H 5 6 AC		4.35 6.60	335.91	41.517	2016.331	2	-0.02	0.001
SEE 271	16 19.3 -42 40	5.83 6.86	114.68	0.407	2016.332	1	-0.42	0.039
COO 197 AB	16 25.3 -49 09	8.11 8.23	91.72	2.369	2016.332	1	-0.35	0.006
H 2 19 AB	16 25.6 -23 27	5.07 5.74	334.40	3.049	2016.335	2	-2.81	0.177
STF 2055 AB	16 30.9 +01 59	4.15 5.15	41.90	1.385	2016.329	1	-0.26	-0.038
I 336	16 31.9 -62 17	7.81 8.14	197.15	1.021	2016.335	1	0.03	-0.004
R 283	16 42.5 -37 05	6.98 7.83	246.11	0.821	2016.331	2	1.18	-0.006
COO 201	16 50.6 -50 03	7.17 7.33	40.07	3.182	2016.335	1	0.38	0.003
STF 2106 AB	16 51.1 +09 24	7.07 8.20	172.40	0.751	2016.329	1	1.47	-0.051
BU 1118 AB	17 10.4 -15 44	3.05 3.27	230.77	0.550	2016.332	3	0.14	-0.004
SHJ 243 AB	17 15.3 -26 36	5.12 5.12	140.50	5.071	2016.333	3	0.13	0.031
MLO 4 AB	17 19.0 -34 59	6.37 7.38	127.02	0.921	2016.340	3	0.17	0.011
BU 416 AC		6.37 10.6	140.95	33.108	2016.340	2	--	--
BSO 13 AB	17 19.1 -46 38	5.61 8.88	257.86	10.480	2016.335	1	-0.04	-0.020
HJ 4931	17 20.6 -59 26	7.76 7.78	254.80	0.799	2016.335	1	--	--
STF 2173 AB	17 30.4 -01 04	6.06 6.17	143.60	0.651	2016.329	1	0.42	-0.009
HLD 136 AB	17 31.7 -41 02	7.81 8.06	107.10	1.026	2016.335	1	--	--
HDO 275	17 44.3 -72 13	6.85 8.11	68.20	0.665	2016.332	1	-3.67	-0.067
STF 2244 *	17 57.1 +00 04	6.89 6.56	100.70	0.659	2016.329	1	-1.20	0.140
RMK 22	17 57.2 -55 23	7.02 7.93	96.20	2.425	2016.335	1	--	--
I 1013	17 58.0 -39 08	6.46 8.19	129.28	1.057	2016.335	1	--	--
STF 2262 AB	18 03.1 -08 11	5.27 5.86	287.90	1.521	2016.329	1	0.34	-0.009
STF 2272 AB	18 05.5 +02 30	4.22 6.17	124.48	6.391	2016.329	1	-0.36	0.009
STF 2281 AB	18 09.6 +04 00	5.97 7.52	285.12	0.711	2016.329	1	2.52	-0.009
HDO 150 AB	19 02.6 -29 53	3.27 3.48	251.77	0.574	2016.359	1	-0.02	-0.012
HN 126	19 04.3 -21 32	7.87 8.06	184.14	1.288	2016.335	2	-0.14	0.005
GLE 3	19 17.2 -66 40	6.12 6.42	349.31	0.518	2016.335	1	-1.59	-0.006
I 253 AB	19 19.0 -33 17	8.77 7.25	140.47	0.470	2016.359	1	-1.19	0.072
SLR 14	23 50.6 -51 42	8.28 8.59	59.22	0.960	2016.355	3	-1.10	0.010

Table notes:
Terms “cpm” (common proper motion) and “relfix” (relatively fixed) refer to Burnham [10].

01 06.1: beta Phoenicis, binary, P = 168 y.

07 38.8: kappa Puppis, relfix, few data, last entry in WDS from 2009.

07 43.0: in Puppis, binary, P = 158.7 y.

07 47.9: in Puppis, binary, P = 1332 y (?)

07 55.8: in Puppis, few data, last entry in WDS from 1996.

08 33.1: in Pyxis, binary, P = 142.9 y, own measures follow trend of recent speckle data, both PA and rho seem to deviate from ephemeris.

08 39.1: in Pyxis, binary, P = 123 y, orbit highly inclined, own measures follow trend of recent speckle data. Significant deviation from ephemeris.

09 30.7: psi Velorum, binary, P = 34 y (?), own measures seem to follow trend of recent speckle data. Significant deviation from ephemeris.

09 32.3: in Vela, difficult, because of large difference in brightness of the components, few data.

09 52.5: gamma Sextantis, binary, P = 77.8 y, own measure of rho deviates from ephemeris, but seems to follow trend of speckle data (last catalog entry from 2011).

10 06.2: in Vela, binary, P = 202.7 y.

10 36.1: in Hydra, binary, P = 158.5 y, positions of components listed in Gaia DR1. Rho value markedly deviates from ephemeris. Own measure close to the value extrapolated from Gaia data.

10 37.3: in Vela, short period binary, P = 16.7 y, both PA and rho start to rapidly decrease in the next years. Own measure of rho deviates from ephemeris, in accordance with recent speckle data.

10 43.3: 35 Sextantis, few data.

10 46.8: mu Velorum, binary, P = 149.3 y, orbit exhibits high eccentricity, measure of rho deviates.

10 49.3: 40 Sextantis, few data with considerable scatter.

10 53.7: in Carina, relfix, PA slowly increasing, few data.

11 17.5: in Carina, relfix, few data, but positions of components are listed in Gaia DR1.

11 23.4: in Musca, few data, PA increasing.

11 27.2: in Crater, binary, P = 48.4 y.

11 28.6: in Centaurus, binary, P = 650 y (?), orbit highly inclined, only few data, significant deviation from ephemeris from 2002, both of own and of recent speckle data.

11 36.6: in Hydra, relfix, cpm, few data, PA decreasing, rho slowly increasing.

11 51.9: in Musca, relfix, rho decreasing, few data.

11 55.0: in Centaurus, binary, P = 930 y (?), orbit highly inclined, few data. Positions of components listed in Gaia DR1. Significant deviations from ephemeris. See fig. 6.

12 04.8: in Crux, wide pair, relfix. Positions of components A and B listed in Gaia DR1.

12 13.6: in Hydra, few data, PA decreasing.

12 15.8: in Corvus, binary, P = 873 y (?), own measure of rho deviates from ephemeris, but seems to follow trend of speckle data.

12 24.9: in Crux, few data, but positions of components are listed in Gaia DR1.

12 26.6: alpha Crucis, few data with some scatter for both AB and AC.

12 28.3: in Crux, binary, P = 2520 y (?). Only short arc on orbit documented. Positions of components are listed in Gaia DR1. Significant deviation from ephemeris from 2002.

12 41.3: in Corvus, few data, PA slowly increasing.

12 41.7: gamma Virginis, binary, P = 169 y, one of three recordings was also evaluated with speckle interferometry. See fig. 3 and table 2.

12 46.3: beta Muscae, binary, P = 194.3 y, measured position significantly deviates from ephemeris values for both PA and rho, in accordance with the trend of recent speckle data.

12 54.6: mu Crucis, few data with some scatter.

12 56.7: in Centaurus, binary, P = 173.4 y, measured position close to ephemeris.

13 03.8: in Virgo, binary, P = 59 y, orbit edge-on, rho rapidly decreasing.

13 14.9: in Virgo, Aa-Ab binary, P = 122.7 y, few data, own measure of rho seems to deviate from ephemeris.

13 34.3: in Virgo, binary, P = 461 y. Positions of components listed in Gaia DR1. Calculated values of PA and rho close to ephemeris, as also own measures.

13 34.7: in Virgo, binary, P = 177.7 y, orbit highly eccentric.

13 43.8: in Virgo, few data, PA and rho decreasing.

13 46.1: in Virgo, binary, P = 261.6 y, many speckle data. Positions of components listed in Gaia DR1. Calculated values of PA and rho slightly deviate from ephemeris.

13 53.5: also known as Y Centauri, AB binary, P = 373 y, own measures are close to recently revised orbit. Few data for AE.

13 55.0: in Virgo, binary, P = 2613 y (?), only short arc on orbit documented, own measures follow trend of speckle data. Rho values deviate from ephemeris.

14 07.7: in Centaurus, binary, P = 336.9 y. Measure of PA close to recently revised ephemeris, but rho tends to deviate.

14 20.2: in Lupus, cpm, relfix, few data, rho decreasing.

14 39.6: alpha Centauri, binary, P = 79.9 y, measures are averaged from nine recordings in seven nights, including two series of speckle images. As a result, the averaged residuals, referred to the interpolated ephemeris by *Pourbaix* from 2016 [8], which are given in the table, exceed the statistical error margins of +/- 0.3 degrees and +/- 0.012 arcsec, respectively. See also fig. 4, and table 2.

14 40.8: in Circinus, few data, but positions of components are listed in Gaia DR1.

14 56.5: in Centaurus, binary, P = 40 y, highly eccentric orbit, own measures deviate from ephemeris (last entry from 1991), but follow trend of speckle data.

14 56.5: in Lupus, relfix, few data, rho decreasing.

15 05.1: pi Lupi, few data, PA slowly decreasing.

15 14.0: in Lupus, few data, but positions of components are listed in Gaia DR1.

15 18.5: mu Lupi, AB: PA & rho decreasing. AC: few data with some scatter.

15 29.5: in Circinus, very few data, but positions of components are listed in Gaia DR1. PA & rho increasing.

15 35.1: gamma Lupi, binary, P = 190 y, orbit highly inclined, many speckle data. Also measured by speckle interferometry. See fig. 5 and table 2.

16 03.5: iota Normae, only few data.

16 03.8: in Lupus, relfix, few data, but positions of components listed in Gaia DR1. PA & rho decreasing.

16 04.4: xi Scorpii, triple system, AB: P = 45.9 y, many speckle data. AC: P = 1514 y (?), only short arc of orbit documented. Positions of A and C are listed in Gaia DR1. Significant deviation from ephemeris.

16 04.4: in Scorpius, few data with some scatter, but positions of components are listed in Gaia DR.

16 12.0: nu Scorpii, “double-double”, but no orbits known. Components A, C, and D are listed in Gaia DR1. Rho(AB), and PA(CD) slowly increasing.

16 19.3: lambda Normae, binary, P = 67.5 y, few data, rho seems to deviate from ephemeris from 2001.

16 25.3: in Norma, binary, P = 1132 y (?), only relatively short arc of orbit documented, positions of components are listed in Gaia DR1.

16 25.6: in Ophiuchus, binary, P = 2398 y, only short arc of orbit documented. Significant deviation from ephemeris.

16 30.9: lambda Ophiuchi, binary, P = 129 y, many visual and speckle data. Own measures follow trends of speckle data. Rho values deviate from ephemeris, at least since 2000.

16 31.9: in Triangulum Australe, few data, but positions of components listed in Gaia DR1. Rho decreasing.

16 42.5: in Scorpius, binary, P = 691 y, few data, no recent speckle data.

16 50.6: in Ara, relfix, few data, but components listed in Gaia DR1.

16 51.1: in Ophiuchus, binary, P = 1270 y (?), orbit highly inclined, many speckle data.

17 10.4: lambda Ophiuchi, binary, P = 87.6 y, many speckle data. See table 2.

17 15.3: 36 Ophiuchi, binary, P = 470.9 y.

17 19.0: in Scorpius, AB binary, P = 42.15 y, PA and rho rapidly decreasing, own measures close to ephemeris. AC: PA and rho increasing.

17 19.1: also known as L 7194, in Ara, binary, P = 953 y. Own measures close to recently revised orbit.

17 20.6: relfix, few data with large scatter, PA decreasing?

17 30.4: in Ophiuchus, binary, P = 46.4 y, orbit highly inclined, many speckle data, rapidly closing in.

17 31.7: in Scorpius, few data.

17 44.3: in Apus, binary, P = 98.6 y, few data.

17 57.1: in Ophiuchus, binary, P = 368 y, orbit highly inclined, own measures follow trend of speckle data, significant deviation of rho from ephemeris. See figs. 7 and 8.

17 57.2: in Ara, few data, PA increasing, rho decreasing?

17 58.0: in Scorpius, few data, PA decreasing, rho increasing.

18 03.1: 69 Ophiuchi, binary, P = 257 y, many speckle data, as well as own measures close to ephemeris.

18 05.5: 70 Ophiuchi, binary, P = 88.4 y, orbit well documented.

18 09.6: 73 Ophiuchi, binary, P = 294 y, many speckle data.

19 02.6: zeta Sagittarii, short period binary, P =21 y.

19 04.3: in Sagittarius, also known as HU 261, binary, P = 500 y, own measures, as well as recent speckle data, are close to positions derived from Gaia DR1, but rho values significantly deviate from ephemeris.

19 17.2: in Pavo, binary, P = 150.8 y, own measures follow trend of speckle data, and are close to ephemeris.

19 19.0: in Sagittarius, binary, P = 60 y, orbit almost edge-on, own measures of rho markedly deviate from ephemeris, in accordance with trend of speckle data.

23 50.6: in Phoenix, binary, P = 135 y.

In figure 1, residuals of separations rho are plotted versus rho. Besides the reference systems (star symbols), only binaries are included (circles with dots), for which residuals refer to the respective ephemeris. Several systems exhibit more or less significant deviations, up to 0.19", far beyond the scale of this plot. Typical reasons for large deviations are "premature" orbit calculations, difficult highly inclined orbits, or general scatter of data. Some noteworthy examples are illustrated in more detail below. In contrast, largest residuals of the reference pairs are about +/- 0.008 arcsec, while the standard deviation is +/- 0.005 arcsec. Limits of the total error margins are represented by curved lines (due to the logarithmic scaling), which are calculated as the sum of the maximum deviations of the calibration pairs, plus the contribution from the error margin of the calibration constant (+/-0.1 per cent), which increases with separation.

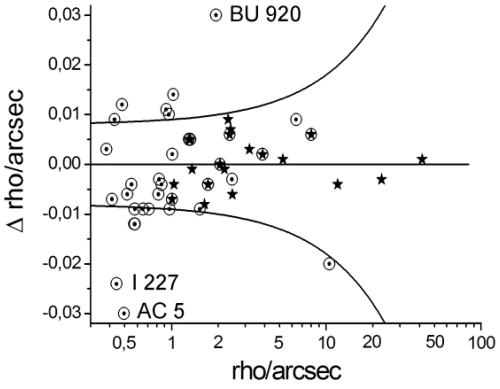

Fig. 1: Plot of the residuals delta rho versus rho. Semi-logarithmic scale. Stars denote reference systems from Gaia DR1, symbols with circles indicate binaries, a few of which are marked with their names. The curves represent maximum error limits. There are several more systems with larger residuals, lying beyond the scale of this plot. See text.

In fig. 2, the residuals of measurements of the position angles are plotted versus the separation rho. It is apparent that the range depends on the separation, and is generally smaller for the reference systems. The reason is the constant resolution of the image, which causes the error of angular measurements to increase towards small separations. It can reach several degrees for systems close to the resolution limit. Also, error margins increase, when a dim companion is lying at or near the diffraction ring of the main star, which makes selection of "lucky" images difficult. For large separations, in particular for the reference systems, the error is of the order of +/- 0.1 to 0.2 degrees as an average, which mainly reflects the error in determining the east-west direction from star trails.

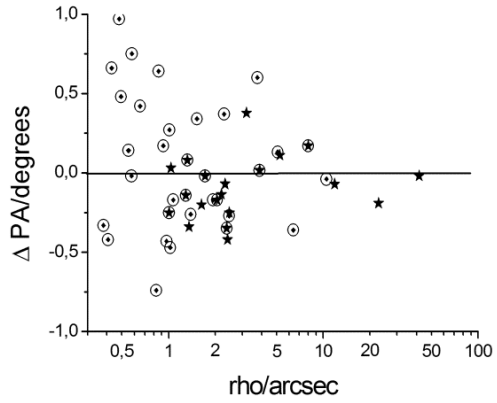

Fig. 2: Plot of the residuals of the position angle PA versus rho. Semi-logarithmic scale. Stars denote reference systems from Gaia DR1, symbols with circles indicate binaries. Generally, the scatter of the residuals increases towards smaller position angles, due to the fixed resolution of the image scale. Residuals of several other systems exceed the scale of this plot. See text.

Speckle Interferometry

Variable seeing conditions produced abundant speckle images, in particular for brighter pairs, which were selected and separately evaluated with the function *autocorrelation*, provided by the program *Reduc* [6]. Three examples are illustrated in figs. 3, 4, and 5.

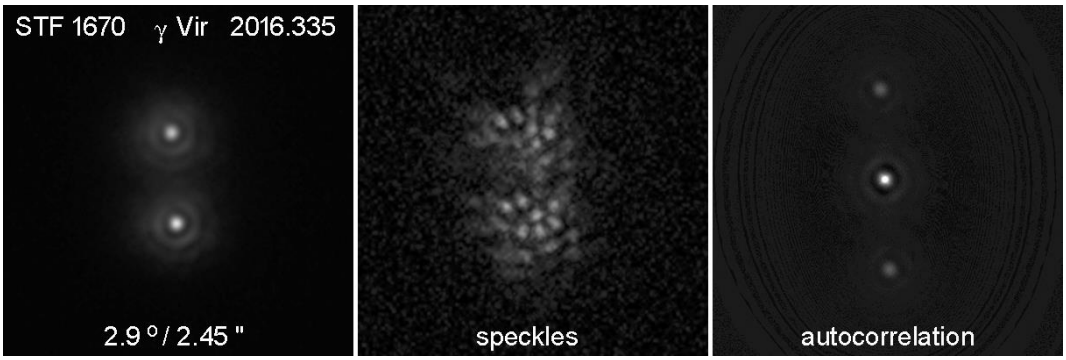

Fig. 3: The binary gamma Virginis. Stack of 94 lucky images, middle: single speckle image (contrast enhanced), right: autocorrelation of 203 speckle images. Exposure time was 5.4 msec. North is down, east is right, as in all images presented in this work.

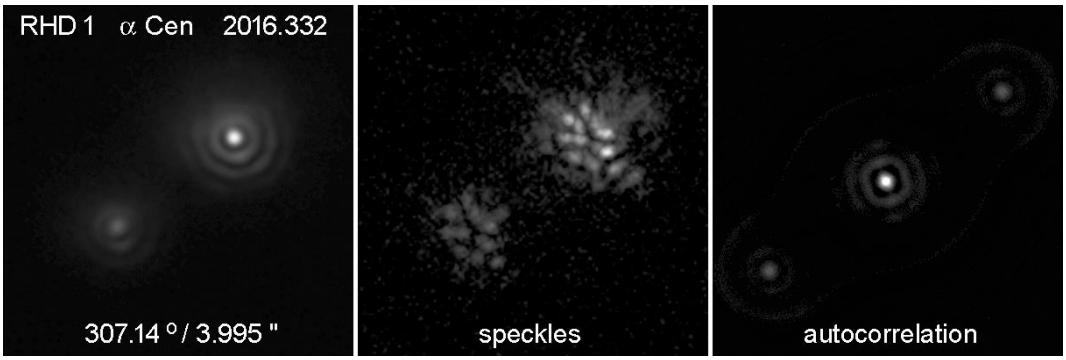

Fig. 4: The binary alpha Centauri. Left: Stack of 97 lucky images, middle: single speckle image (contrast enhanced), right: autocorrelation of 234 speckle images. Exposure time was 0.25 msec.

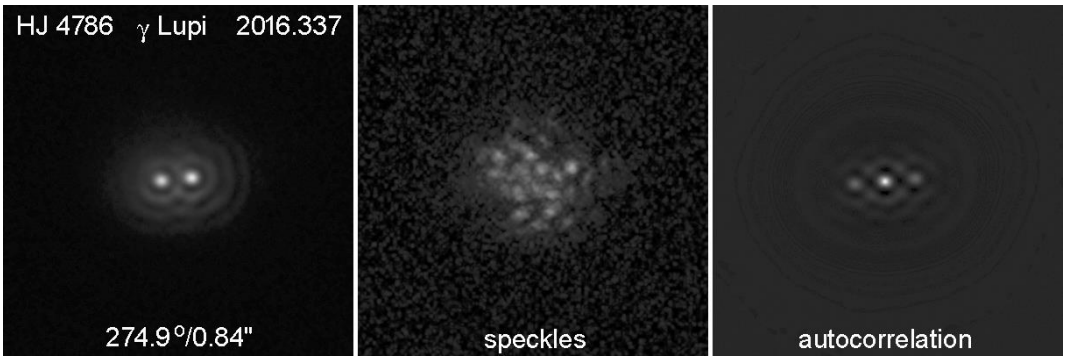

Fig. 5: The binary gamma Lupi. Left: Stack of 89 lucky images, middle: single speckle image (contrast enhanced), right: autocorrelation of 150 speckle images. Exposure time was 5.4 msec.

Measurements for nine pairs are compared with lucky imaging of the same systems in table 2. Position angles and separations do not differ by more than 0.8 degrees, or 0.01 arcsec, with mean values of the order of 0.1 degrees, and below 0.001 arcsec, respectively. These figures correspond to the error margins stated above. As a conclusion, the accuracy of both methods is virtually the same, which is expected, because both are based on images with the same optics.

Table 2: Position measurements for 9 pairs with speckle interferometry and lucky imaging. Column "RA" contains right ascension values for identification. For several pairs, two and more recordings have been evaluated, as indicated below the table. Results from autocorrelation are included in the mean values given in table 1. See also notes to table 1.

PAIR	RA	PA/deg	rho/"	PA/deg	rho/"	Δ PA	Δ rho	common
		autocorrelation		lucky imaging		deg	arcsec	name
DUN 252 AB	12 26.6	111.81	3.891	[X] 111.68	[X] 3.897	+0.13	-0.006	alp Cru
STF 1670	12 41.7	2.84	2.451	* 3.00	* 2.457	-0.06	-0.006	gam Vir
R 207	12 46.3	52.94	1.010	* 53.52	* 1.002	-0.58	+0.008	bet Mus
RHD 1	14 39.6	* 307.39	* 3.994	[#] 307.21	[#] 3.999	+0.18	-0.005	alp Cen
HJ 4753 AB	15 18.5	298.45	0.772	298.99	0.775	-0.54	-0.003	mu Lup
HJ 4786	15 35.1	* 275.38	* 0.827	* 275.66	* 0.829	-0.28	-0.002	gam Lup
STF 1998	16 04.4	6.17	1.096	* 6.11	* 1.098	+0.06	-0.002	xi Sco
H 2 19 AB	16 25.6	334.38	3.054	334.41	3.044	-0.03	+0.010	in Ara
BU 1118 AB	17 10.4	231.13	0.554	* 230.77	* 0.550	+0.36	+0.004	eta Oph

*: mean of 2 recordings; [X]: mean of 4 recordings; [#]: mean of 7 recordings.

Discussion

In several cases of binaries, data from Gaia reveal and/or confirm deviations from currently assumed orbits. An example is the system HLD 114 in Centaurus (RA 11 55.0), which is illustrated in figures 6 a) and b). The orbit is highly inclined, and the companion does not move as expected, such that the difference of the separation from the ephemeris has increased to about 0.9 arcsec. Other binaries, for which positions from Gaia markedly deviate from ephemeris data, but more or less agree with trends of speckle and own measures, are BU 411 in Hydra (10 36.1), CPO 12 in Crux (12 28.3), STF 1781 AB in Virgo (13 46.1), STF 1998 AC in Scorpius (16 04.4), COO 197 in Norma (16 25.3), and HN 126 in Sagittarius (19 04.3).

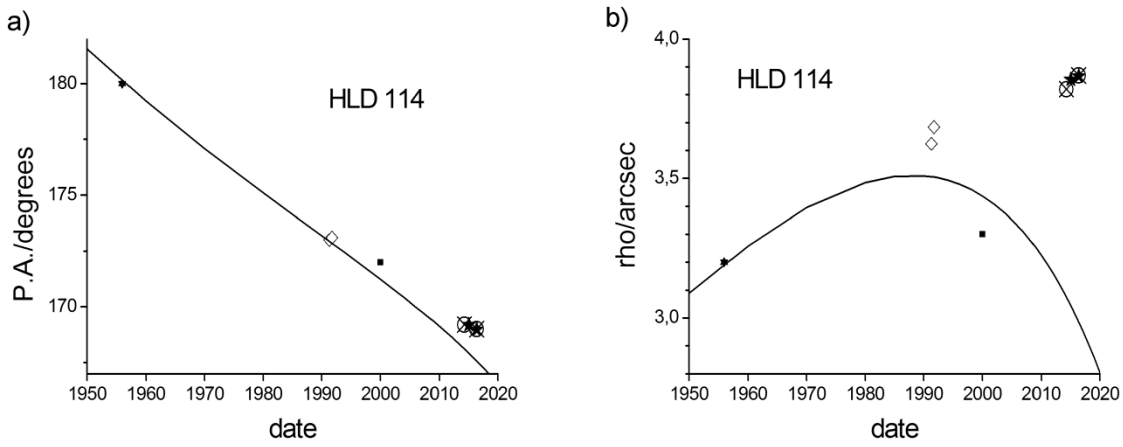

Fig. 6 a): Plot of the position angle of HLD 114 vs. time. Open rhombs indicate speckle data, crossed circles own measurements, a full square is from the WDS, a small star from the Sky Catalogue 2000.0. Large stars represent the results from Gaia for the epoch 2015.0, and extrapolated to 2016.337. Curves are the ephemeris. b): Plot of the separation rho vs. time. See also note 11 55.0 above.

A rather similar example is the binary STF 2244 in Ophiuchus, an image of which is shown in fig. 7. Again, the orbit is highly inclined, and the companion should have turned around already, but has continued to move straightforward. This is revealed by many speckle data, as well as my own measures in 2014 and 2016. The separation is now off the ephemeris by about 0.14 arcsec, clearly beyond all error margins, as can be seen in the plot in figure 8. See also note 17 57.1 above.

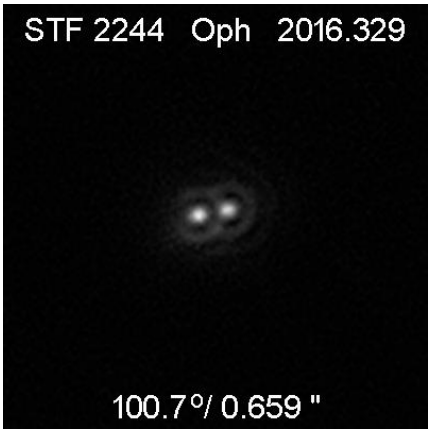

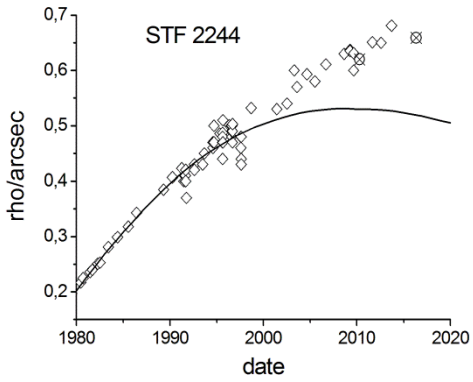

Fig. 7 (left): The binary STF 2244 in Ophiuchus. Stack of 70 best frames. Exposure was 50.3 msec.
Fig. 8 (right): Plot of the separation rho vs. time. Open rhombs are speckle data, crossed circles are own measures, and the curve is the ephemeris.

For a better overview, in the following table all binaries are listed, for which more or less significant deviations of their positions from currently assumed ephemeris data have been found or confirmed:

Pair	RA+Dec	Name and/or Constellation	Remarks
BU 205 AB	08 33.1 -24 36	Pyxis	
BU 208 AB	08 39.1 -22 40	Pyxis	orbit highly inclined
COP 1	09 30.7 -40 28	psi Velorum	
AC 5 AB	09 52.5 -08 06	gamma Sextantis	

BU 411	10 36.1 -26 41	Hydra	confirmed by Gaia
SEE 119	10 37.3 -48 14	Vela	
I 885 AB	11 28.6 -45 08	Centaurus	orbit highly inclined
HLD 114	11 55.0 -56 06	Centaurus	orbit highly inclined, confirmed by Gaia
CPO 12 A,BC	12 28.3 -61 46	Crux	confirmed by Gaia
R 207 AB	12 46.3 -68 07	beta Muscae	
STF 1781 AB	13 46.1 +05 07	Virgo	confirmed by Gaia
STF 1788 AB	13 55.0 -08 04	Virgo	
SLR 19	14 07.7 -49 52	Centaurus	
RHD 1 AB	14 39.6 -60 50	alpha Centauri	deviation small, but distinct
I 227 AB	14 56.5 -34 38	Centaurus	
STF 1998 AC	16 04.4 -11 22	xi Scorpii	confirmed by Gaia
SEE 271	16 19.3 -42 40	lambda Normae	
COO 197 AB	16 25.3 -49 09	Norma	confirmed by Gaia
H 2 19 AB	16 25.6 -23 27	Ophiuchus	
STF 2055 AB	16 30.9 -01 59	lambda Ophiuchi	
STF 2244	17 57.1 +00 04	Ophiuchus	orbit highly inclined
HN 126 AB	19 04.3 -21 32	Sagittarius	confirmd by Gaia
I 253 AB	19 19.0 -33 17	Sagittarius	

Conclusion

A major improvement of the accuracy of double star measurements was possible by calibrating the image scale with reference stars, for which the recently published first Gaia catalog provides extremely precise position data. The error margin of the resulting scale factor was estimated to below +/-0.1 per cent. This is much lower than previous values, which were based on double star data from catalogs, which exhibit more or less large scatter. The remaining statistical scatter of separation measurements of below +/-0.01 arcsec is mainly caused by seeing effects, and by the limited resolution of the telescope. This accuracy is much better than the Rayleigh limit, which, however, merely characterizes the splitting power of close doubles.

The seeing was rather variable during this stay, and produced many periods of speckle images. This offered the opportunity to directly compare the precision of lucky imaging and speckle interferometry. As a result, error margins were found to be of the same order. This is expected, because both methods are based on images obtained with the same optics.

For only 20 of the 95 systems investigated here, positions could so far be found in the present Gaia catalog. Residuals either refer to this data, or to ephemeris data of binaries. For most other systems, no residuals are given, because the scatter of literature data was found too large, as to allow reasonable extrapolations to the date of own measurements.

Several binaries were found with positions deviating from the respective ephemeris. This was confirmed either by data from Gaia, and/or by trends of recent speckle measurements (within the estimated error limits). For the other pairs, for which mostly only few data could be found in the literature, it is hoped that the present measurements may help to improve the knowledge about their status.

Acknowledgements

This work has made use of data from the double star catalogs provided by the United States Naval Observatory, as well as data from the Gaia satellite mission, which were recently published by the ESA consortium. Thanks are also due to Florent Losse for providing his program *Reduc*.

References

[1] Anton, R., Lucky Imaging, in *Observing and Measuring Visual Double Stars*, 2nd edition, Robert Argyle, ed., Springer New York 2012.

[2] Turner, N., Astrometric Speckle Interferometry for the Amateur, in *Observing and Measuring Visual Double Stars*, 2nd edition, Robert Argyle, ed., Springer New York 2012.

[3] Gaia Archive, Data release 1: http://esac.esa.int/archive/, online access Dec. 2016.

[4] IAS, http://www.ias-observatory.org

[5] Anton, R., 2015, *Journal of Double Star Observations*, vol. 11(2), 81-90.

[6] Losse, F., http://www.astrosurf.com/hfosaf

[7] Mason, B.D. et al., *The Washington Double Star Catalog (WDS)*, U.S. Naval Observatory, online access Jan. 2017.

[8] Hartkopf, W.I. et al., *Sixth Catalog of Orbits of Visual Binary Stars*, U.S. Naval Observatory, online access Jan. 2017.

[9] Hartkopf, W.I. et al., *Fourth Catalog of Interferometric Measurements of Binary Stars*, U.S. Naval Observatory, online access Jan. 2017.

[10] R. Burnham, *Burnham´s Celestial Handbook*, Dover Publications, New York 1978.